Adaptive Subcarrier-Bandwidth Multiple Access (ABMA) for High-Mobility Environments

Jionghui Li(✉), Xiongwen He, Xiaofeng Zhang, and Fan Bai

Beijing Institute of Spacecraft System Engineering, Beijing 100094, China
lijionghui@126.com

Abstract. In this paper, adaptive subcarrier-bandwidth multiple access (ABMA) is proposed as a novel downlink multi-user access scheme to support robust wireless communications in the high-mobility environments with different kinds of high-speed receivers. The proposed ABMA allows flexible spectrum resource allocation and subcarrier bandwidth adaptation according to mobile receivers' velocities. Resource band is used as the unit for spectrum resource allocation. Well-localized band-pass filters are applied on each resource band, in order to control the multiple access interference and achieve coexistence of different subcarrier bandwidth. Universal receiver structure with low implementation complexity is described as part of the scheme. Theoretical and numerical results show that the ABMA scheme is effective in repelling the impact of high-range Doppler effects and performs high robustness in the high-mobility environments.

Keywords: Adaptive subcarrier-bandwidth multiple access · High-mobility · Doppler effects

1 Introduction

With the development of integrated space-ground networks and internet of things (IoT), future space links should provide communication services for different kinds of ground users, including planes, vessels, high-speed trains, ground vehicles and individual pedestrians. Therefore, future space-ground network is expected significant improvement over current space links on peak data rate and high scalability. This requires the space-ground downlink transmission system to support a wide range of user velocities over 500 km/h (for civil aviation and high-speed train). Additionally, future integrated space-ground networks are targeted to unified transmission systems for ground and space as well as better spectral efficiency to support high volumes of signaling and data transmission. These bring challenges to current orthogonal frequency-division multiple access (OFDMA) systems, since the OFDM signal is sensitive to inter-carrier interference (ICI) caused by the Doppler effects with the high-speed relative movement.

M. Jia et al. (Eds.): WiSATS 2019, LNICST 280, pp. 475–486, 2019.
https://doi.org/10.1007/978-3-030-19153-5_49

Regarding to a large scale of users with different channel conditions and time-varying moving velocities, downlink transmission signal should be robust and flexible for user-specific environments in order to serve such large-scale multi-user access in the high-mobility environments, providing a supportive technique for future development of integrated space-ground networks and IoT. Universal-filtered multicarrier (UFMC) [1] and filtered-OFDM (f-OFDM) [2] are developed as subband-based filtered waveforms which provide better spectrum localization compared to conventional OFDM and keep relatively balance with time localization compared with filter band multi-carrier (FBMC). Although subband-based spectrum localization helps to reduce multiple access interference (MAI) from other subbands, the improvement on the overall inter-carrier interference (ICI) is still limited, since the ICI mainly comes from the adjacent subcarriers within the subband. ICI is proportional to the maximum Doppler shift, whereas it is inversely proportional to the subcarrier bandwidth. Therefore, subcarrier bandwidth is proposed to be considered as a system freedom. [3] discusses different subcarrier bandwidths for OFDMA systems over fast fading channel. [4] and [5] have highlighted user-specific subcarrier spacings with UF-OFDM to improve low latency and high Doppler use cases in an uplink model, allowing users to pick up different settings for its signal. Compared to UFMC, Filtered-OFDM has even lower out-of-band emission (OOBE). Therefore, filtered-OFDM waveform allows for a minimum number of guard tones between each subband [2], making it flexible for coexistence of different settings in each subband to acquire frequency domain quasi-orthogonality. A downlink transceiver structure of filtered-OFDMA is introduced in [6], which applies user-specific subcarrier spacing, cyclic prefix (CP) length, transmission time interval (TTI) duration and spectrum shaping filters. Further considering the time-varying cases, Doppler frequency shift becomes hard to estimate ahead of time. Therefore, to ensure the multi-user downlink transmission robustness, spectrum resource adaptive allocation should be applied based on the feedback of channel and users' information. The current multi-user access schemes are designed with constant parameters, which are not flexible enough to support the time-varying scenarios. Hence, a new multi-carrier access with flexible spectrum resource allocation and subcarrier bandwidth adaptation is demanded for downlink multiuser transmissions, to serve high scale users in time-varying high-mobility environments. In this paper, we target at time-varying environments where users are moving with a large range of velocities and propose a downlink multi-user access scheme based on filtered-OFDM waveform, named adaptive subcarrier-bandwidth multiple access, ABMA. The targeted problem is addressed in Sect. 2. ABMA scheme and corresponding signal model are introduced in Sect. 3, including the time-spectrum resource allocation, transceiver structure with universal receiver and ICI analysis. Based on the proposed scheme, the numerical results in Sect. 4 prove the high transmission robustness of ABMA system with time-varying Doppler spread in the high-mobility environments. We conclude the paper in Sect. 5.

2 Problem Statement

The average moving velocity of civil aviation aircraft is about 500–1000 km/h. And the average velocities are about 500–600 km/h for vessels, about 300–500 km/h for speed train, 30–200 km/h for cars and up to 10 km/h for pedestrians. Future integrated space-ground networks and IoT are target to support users with such a wide range of velocities. Therefore, Doppler spread is rising compared to that with current settings. The Doppler frequency shift is also time-varying, making it hard to estimate ahead of time. Therefore, signal with higher robustness and less sensitivity to the Doppler effects becomes highly preferred.

For an OFDM-based symbol, the symbol period T follows

$$T = \frac{N + L_{cp}}{B} = \left(1 + \frac{L_{cp}}{N}\right)\frac{N}{B} = (1 + \alpha_{cp})\, f_s \tag{1}$$

where L_{cp} is the length of CP used in OFDMA symbol for ISI elimination, α_{cp} denotes the ratio of CP compared with N, B is the signal bandwidth and the subcarrier spacing $f_s = B/N$.

Then, as derived in [7], in the time-varying Rayleigh fading channel, the ICI power with unit average transmitted signal power is bounded with

$$\begin{aligned} P_{ICI} &\geq \frac{\alpha_1}{12}\left(2\pi f_m T\right)^2 - \frac{\alpha_2}{360}(2\pi f_m T)^4 \\ &= \frac{\alpha_1}{12}\left[2\pi(1+\alpha_{cp})\frac{f_m}{f_s}\right]^2 - \frac{\alpha_2}{360}\left[2\pi(1+\alpha_{cp})\frac{f_m}{f_s}\right]^4 \end{aligned} \tag{2}$$

$$P_{ICI} \leq \frac{\alpha_1}{12}\left(2\pi f_m T\right)^2 = \frac{\alpha_1}{12}\left[2\pi(1+\alpha_{cp})\frac{f_m}{f_s}\right]^2 \tag{3}$$

where f_m is the maximum Doppler frequency with $f_m = \frac{v}{c} f_c$. v is the mobile UE velocity, c is the speed of light and f_c is the RF carrier frequency.

Therefore, from (2)–(3), ICI resulting from Doppler spread is determined by f_m/f_s. We define

$$f_\delta = \frac{f_m}{f_s} \tag{4}$$

as normalized Doppler carrier frequency offset (D-CFO), which is proportional to f_m and inversely proportional to f_s.

Assuming Rayleigh fading channel following Jakes model, $\alpha_1 = 1/2$ and $\alpha_2 = 3/8$ in (2)–(3). Accordingly, for $f_c = 6$ GHz, the ICI power with different receiver velocities is shown in Fig. 1.

Regarding to the downlink transmission, each user may have different time-varying velocities and receive the same transmitted signal with different channel impacts. If the entire OFDM signal parameters are adaptively changed, all the serving users in the cell have to make adjustments accordingly, which is

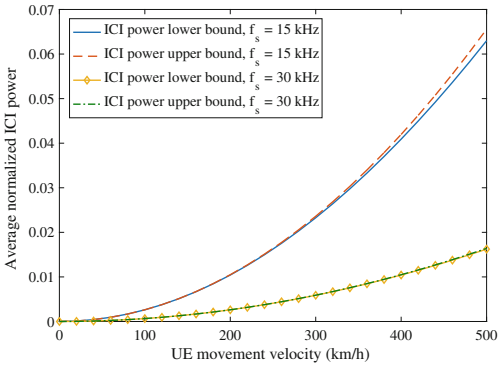

Fig. 1. Comparison of ICI power bounds with different subcarrier spacings at different velocities.

unnecessary for most of the users. Therefore, an efficient adaptation should be conducted on a user basis, instead of on the entire signal setting. In order to satisfy the transmission quality for a large amount of users with temporal channel variations, we need an adaptive scheme that allows dynamic coexistence of different subcarrier bandwidths in one transmitted multi-carrier symbol. The rest of the paper will introduce the proposed novel downlink multi-user access scheme, ABMA, targeting on this issue.

3 Downlink Adaptive Numerology Filtered Multi-carrier Access Scheme

We assume that perfect feedback of the channel state information (CSI) is available at the base station (BS). The BS obtains users' GPS information, including the velocities to decide the spectrum resource allocation.

The subcarrier bandwidth is regarded as $2f_s$. The existing of subcarriers with different bandwidth breaks the orthogonality. Thanks to filtered-OFDM waveform [6], spectrum side lobes are suppressed with subband-based filtering to achieve quasi-orthogonality in the frequency domain, allowing different bandwidths. ABMA scheme is designed based on filtered OFDM waveform. However, as a multiple access scheme, ABMA is different from the filtered-OFDMA [2] in the following aspects:

1. In filtered-OFDMA scheme, user data are allocated on a subband basis. With different subcarrier spacing, the number of subcarriers in each subband varies to keep a relative constant subband width. To differentiate from the concept of subband, in the ABMA scheme, we use the concept of "resource band (Rb)" as the unit of filtering and user resource allocation. For reception and allocation convenience with the adaptive scheme, each resource band loads a fixed number of subcarriers, while the signal bandwidth of the resource band varies with difference subcarrier spacing settings.

2. The resource allocation and parameters setting can be variable for each TTI in ABMA, while filtered-OFDMA applies the constant settings.
3. In order to minimize the transmission overhead and guard tones, in each time unit, BS pre-allocates the resource bands into groups based on the bandwidth. In each group, consistent parameters is applied.
4. In the proposed ABMA scheme, each receiver-end is able to locate the resource band based on the adaption control information and to demodulate the user data with an universal structure, instead of using matched filters as filter-OFDMA. The filter banks are avoided for better supporting the adaptation with reasonable implementation complexity.

3.1 Time-Spectrum Resource Adaptive Allocation

The time-spectrum resource adaptive allocation is illustrated in Fig. 2. As mentioned above, resource band is defined as the spectrum allocation unit. And the transmission time interval (TTI) is the time unit for the adaptation. The waveform setting remains consistent within one TTI.

Each user's data takes one resource band with fixed number of subcarriers, N_s. The resource band allocation for each user is based on the feedback of CSI and the user's GPS information.

The LTE setting with subcarrier spacing, $f_{s1} = 15\,\text{kHz}$, is used as a baseline [4]. Resource bands with baseline setting are used to serve stationary and slow-moving users. With higher velocities, users' are able to request an increment of subcarrier spacing to reduce the ICI caused by Doppler carrier frequency offset (D-CFO). In order to pack all users data into the downlink transmission frame, the adjusted subcarrier spacing should be an integer times of the baseline spacing, i.e. $f_{sz} = r_z \cdot f_{s1}$, where $r_z = 2^{z-1}, z \in \mathbb{Z}^+$. z denotes group index, and r_z is named adjust order.

Receivers depend on the adaptive control information to locate the allocated resource band. In order to minimize the control information overhead and reduce inter-band interference, in each TTI, resource bands are allocated into groups. Each resource band can be defined with three indices, which are resource band index I_b, in-group index I_g and group index z. I_b denotes the order of the resource band regarding to the whole spectrum; I_g reveals the position of the resource band in its group; and z decides the adjust order r_z of the group.

In the example shown in Fig. 2, two subcarrier spacings are applied, which are the baseline spacing $f_{s1} = 15\,\text{kHz}$, and the adjusted spacing $f_{s2} = 30\,\text{kHz}$. At the TTI t_1, $N_{g1}^{t_1}$ number of resource bands keep the baseline spacing and $N_{g2}^{t_1}$ number of resource bands are adjusted to 30 kHz. A slow-moving user, as denoted as U_1 requires downlink transmission. The BS allocates the resource band with $I_b = i$ to transmit the data to U_1. As shown in the figure, it is also the last resource band in the baseline setting group. Therefore, at TTI, t_1, the resource band for U_1 can be defined by $I_b^{t_1} = i$, $I_g^{t_1} = N_{g1}^{t_1}$, and $z = 1$.

At the TTI, t_2, with time-varying motion, the velocity of U_1 is assumed to exceed a pre-settled threshold, ϕ_v. Then, according to the user's GPS information, BS decides to use the adjusted spacing for U_1 data. Thus, the resource band

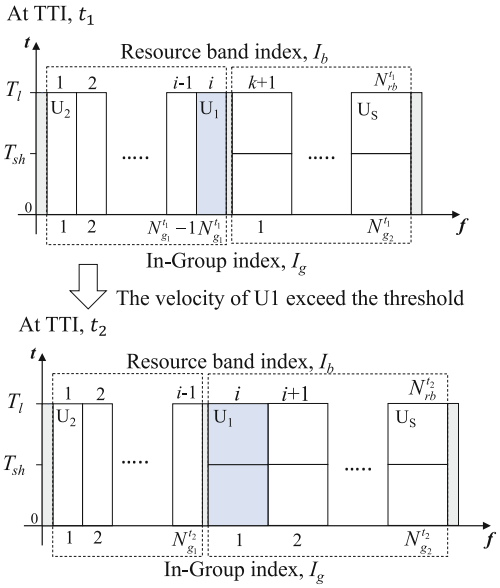

Fig. 2. Illustration of resource band adaptive allocation in two different TTI.

is re-allocated as shown in Fig. 2. The resource band is in one adjusted group, defined by $I_b^{t_2} = k$ and $I_g^{t_2} = 1$. With the same sampling rate, the duration of multi-carrier modulated symbol to U_1 is shortened from T_l to T_{sh}. Guard tones are inserted between each two groups to eliminate inter-band interference.

With the information of z, I_b and I_g, resource bands can be located by calculating the digital domain offset as

$$S_{I_b} = (I_g - 1)N_s + S_{GT} \cdot (z - 1) + \left\lceil \frac{S_{GB} + (I_b - I_g)N_s}{r_z} \right\rceil \tag{5}$$

where S_{GB} denotes the null subcarriers offset as guard bands before the first resource band, and S_{GT} is the offset of guard tones inserted before groups.

With larger subcarrier spacing, the transmitted signal takes more bandwidth resource. In order to keep the scalability with limited bandwidth and keep the long-term balance, the subcarrier spacing should return to baseline once the adjustment is no longer required.

3.2 Downlink Transmitter Structure and Signal Model

Figure 3 depicts the downlink transmitter structure of the proposed ABMA scheme at the TTI t_1, matched with the example shown in Fig. 2.

Mapping to the digital domain, the subcarrier bandwidth/spacing is decided by the length of IFFT. As shown in Fig. 3, let N_1 denote the IFFT length of baseline setting. Then with the adjusted setting, the IFFT length is $N_z = N_1/r_z$.

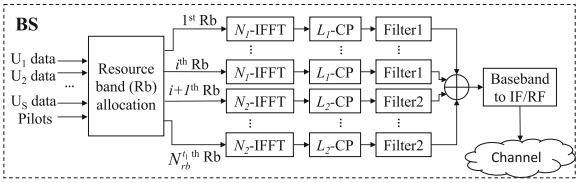

Fig. 3. Downlink transceiver structure at TTI t_1. Baseline setting and one adjusted setting are applied, i.e. $z = 1, 2$.

Regarding to the TTI t_1, if resource band, $I_b = k$, is in the baseline group ($z = 1$) with subcarrier spacing f_{s1}, let $\boldsymbol{X^k} = [X_0^k, X_1^k, \ldots, X_{N_s-1}^k]$ denotes the complex mapped data symbols (including pilots) that will be demodulated into this resource band, then the time-domain output of the IFFT is

$$x^k[n] = \frac{1}{\sqrt{N_1}} \sum_{l=0}^{N_s-1} X_l^k \mathrm{e}^{j2\pi(l+S_k)n/N_1} \tag{6}$$

where $S_k + N_s \leq N_1$. The baseline setting of CP length is denoted as L_1. CP is inserted to $\boldsymbol{x^k}$ for ISI elimination and filter tails treatment. Thus, in (6), $-L_1 \leq n \leq N_1 - 1$.

Then the time-domain signal $\boldsymbol{x^k}$ is filtered by a L_{f1}-length FIR-filter, $\boldsymbol{p_1^k}$ to suppress the spectrum side lobes. The output signal can be expressed as

$$\boldsymbol{s^k} = \boldsymbol{x^k} * \boldsymbol{p_1^k} \tag{7}$$

where $*$ denotes the linear convolution. $\boldsymbol{p_1^k}$ fits to the baseline resource band bandwidth and matches with the central frequency of the resource band.

If resource band $I_b = k$ is in an adjusted group with subcarrier spacing f_{sz}, where $z \neq 1$, The frequency-domain complex mapped data symbols is defined as $\boldsymbol{X^k} = [X_{1,0}^k, X_{1,1}^k, \ldots, X_{1,N_s-1}^k \ldots X_{z,0}^k, X_{z,1}^k, \ldots, X_{z,N_s-1}^k]$. The time-domain output signal is denoted as $\boldsymbol{x^k} = [\boldsymbol{x_1^k}, \ldots, \boldsymbol{x_z^k}]$, where

$$x_z^k[n] = \frac{1}{\sqrt{N_z}} \sum_{l=0}^{N_s-1} X_l^k \mathrm{e}^{j2\pi(l+S_k)n/N_z} \tag{8}$$

with $-L_z + (z-1) \cdot (N_z - 1) \leq n \leq z \cdot (N_z - 1)$, where $N_z = N_1/r_z$. Then, the output signal is

$$\boldsymbol{s^k} = [\boldsymbol{x_1^k} * \boldsymbol{p_z^k}, \ldots, \boldsymbol{x_z^k} * \boldsymbol{p_z^k}] \tag{9}$$

where $\boldsymbol{p_z^k}$ is the L_z-length FIR filter that fits to the adjusted resource band width and matches with the central frequency of the resource band k.

In order to be compatible with transmission frame structure, we desire that $L_z = L_1/r_z$. Therefore, to keep performance of filter tails treatment, the length

of the FIR filter, L_{fz}, is desired to follow $L_{fz} = L_{f1}/r_z$. This is one of the reasons to adjust the bandwidth of resource bands, instead of the subcarrier number within the resource band. With larger passband width, FIR filter can be designed with shorter length to match with the time-domain requirement. Therefore, the transmitted multi-carrier symbol is the superposition of the time-domain modulated symbols corresponding to all of the resource bands, which can be written as

$$s_t[n] = \sum_{k=1}^{N_{rb}^{t_1}} s^k[n], \quad -L_1 \leq n \leq N_1 - 1 \tag{10}$$

where $N_{rb}^{t_1}$ denotes the total number of the allocated resource bands in the TTI t_1. It is seen that the length of the transmitted symbol, $s_t[n]$, is determined by the baseline setting.

3.3 Universal Receiver Structure and Received Signal

To achieve adaption, at the TTI t_1, a certain user, denoted as U_1, should be able to demodulate its data with a universal structure. Parameters can be adjusted according to adaption control information, $(z, I_g^{t_1}, I_b^{t_1})$. Note $I_b^{t_1} = i$. As shown in Fig. 4, at the receiver-end, after down-conversion, synchronization and A/D sampling, CP is discarded and the discrete signal is demodulated by FFT according to the knowledge of z. And based on the information of S_i, corresponding resource band can be located to obtain the U_1 data. S_i can be calculated by (5). Filtering distortion is further compensated by equalization.

Assuming ideal carrier synchronization and sampling rate, the received baseband discrete signal can be written as

$$y[n] = \sum_{\gamma=0}^{\Gamma-1} h[n, \gamma] s_t[n - \gamma] + w[n] \tag{11}$$

where $w[n]$ is additive white Gaussian noise (AWGN) with variance of σ_n^2, and $h[n, \gamma]$ is the channel impulse response of the lth path at sampling time n.

z number of modulated symbols can be successively demodulated from one transmitted symbol. For each modulated symbol, the lth subcarrier within the resource band i can be obtained by FFT as

$$Y_l^i = \frac{1}{\sqrt{N_z}} \sum_{n=0}^{N_s-1} y[n] \mathrm{e}^{-j2\pi n(l+S_i)/N_z} \tag{12}$$

$$= \frac{1}{N_z} X_l^i P_r^i[l] \sum_{n=0}^{N_z-1} H_{l+S_i}[n] + I^i[l] + W^i[l] \tag{13}$$

where $\boldsymbol{P_r^k}$ is the frequency response of FIR filter $\boldsymbol{p_r^i}$ and $W^i[l]$ is the FFT of noise $w[n]$. $I^i[l]$ is the intra-band ICI and inter-band interference. With the filtering,

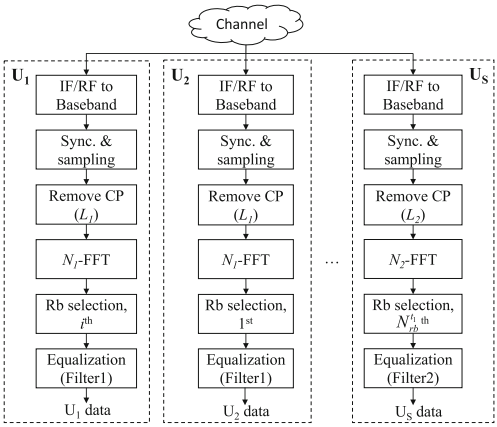

Fig. 4. Downlink receiver structure at TTI t_1. Baseline setting and one adjusted setting are applied, i.e. $z = 1, 2$. Data to U_1 and U_2 are modulated to baseline resource bands $I_b = i$ and $I_b = 1$ respectively, with $z = 1$; and data to U_3 are modulated to the last resource band, $I_b = N_{rb}^{t_1}$, in the adjusted group ($z = 2$).

inter-band interference is negligible compared with intra-band ICI. So, $I^i[l]$ can be written as

$$I^i[l] = \frac{1}{N_z} \sum_{m=0, m\neq l}^{N_s-1} X_m^i P_r^i[m] \sum_{n=0}^{N_z-1} H_{m+S_i}[n] \mathrm{e}^{j2\pi n(m-l)/N_z} \tag{14}$$

Considering the time-varying Rayleigh fading channel following classical Jakes model, we have [8]

$$E\{H[n]H^*[m]\} = J_0\left(2\pi f_m T_z (n-m)/N_z\right) \tag{15}$$

$$= J_0\left(2\pi(1+\alpha_{cp})\frac{f_m}{f_{sz}}(n-m)/N\right) \tag{16}$$

where $J_0(\cdot)$ is the zeroth-order Bessel function of the first kind, $T_z = (1+\alpha_{cp})f_{sz}$ is the modulated symbol duration. Therefore, with $E\{|X_m^i|^2\} = 1$, the average power of ICI is [8]

$$E\left\{\left|I^i[l]\right|^2\right\} = \frac{1}{N_z^2} \sum_{m=0, m\neq l}^{N_s-1} \left[N_z + 2 \sum_{n=1}^{N_z-1} (N_z - n) J_0\left(2\pi f_m T_s n\right) \cdot \cos\left(\frac{2\pi n(m-l)}{N_z}\right)\right] \tag{17}$$

Figure 5 shows the signal-to-ICI ratio (SIR) under different user movement velocities. A comparison is made between baseline OFDMA and ABMA with $z = 1, 2, 3$.

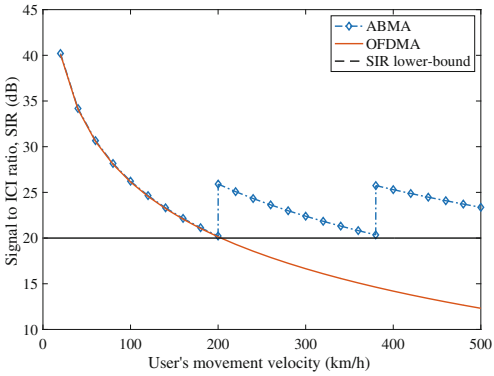

Fig. 5. Signal-to-ICI ratio comparison between baseline OFDMA and ABMA. Subcarrier spacings of ABMA switch among three settings with $z = 1, 2, 3$ to ensure the SIR above the required lower-bound.

For illustration purpose, we set a required SIR lower-bound to 20 dB. It is seen from Fig. 5 that only 200 km/h can be supported with SIR above the lower-bound by baseline OFDMA. While with ABMA, it is able to remain the SIR above the required SIR by its adaptive structure. Thus, ABMA can be much more robust than OFDMA in the time-varying mobility environments with high-range velocities.

4 Numerical System Evaluation

In this section, we present the numerical system evaluation. RF carrier frequency is set to be 6 GHz. Users' velocities are time-varying in the range of 0 to 500 km/h with uniform distribution. Perfect CSI and users' GPS information is assumed to be available at the BS. One adjusted numerology setting is applied, i.e. $z = 1$ or 2, as summarized in Table 1. For simulation purpose, set the pre-settled velocity threshold, $\phi_v = 260$ km/h. Considering the balance of frequency-time localization, soft-truncated sinc filters with Hanning window [6] is used as the prototype of FIR bandpass filters for each resource band. Guard tones between the two groups is 4×30 kHz. Figure 6 shows the BER performance

Table 1. Simulation parameters of ABMA.

Parameter	Baseline setting	Adjusted setting
Resource band size, N_s	60	60
Subcarrier spacing	$f_{s1} = 15$ kHz	$f_{s2} = 30$ kHz
Length of IFFT/FFT	$N_1 = 2048$	$N_2 = 1024$
Filter length	$L_{f1} = 200$ samples	$L_{f2} = 100$ samples
CP length	$L_1 = 160$ samples	$L_2 = 80$ samples

with QPSK data symbols in Rayleigh channel following classical Jakes model and a line-of-sight transmission, under OFDMA and proposed ABMA respectively. Zero-forcing equalization is used to compensate the filtering distortion. Three pilots are inserted in each resource band for phase tracking.

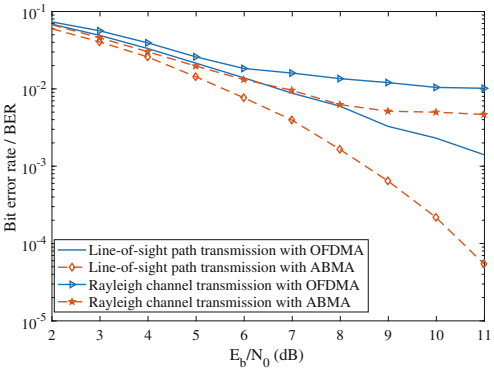

Fig. 6. BER performance of ABMA and OFDMA in time-varying mobility environment, with $z = 1, 2$; $\phi_v = 260$ km/h.

Compared to baseline setting OFDMA, ABMA brings 3 dB E_b/N_0 gain for BER $= 10^{-3}$ regarding to the line-of-sight path transmission as well as lower BER platform with Rayleigh channel. The results prove that ABMA enhances the transmission robustness in time-varying mobility environment with high-range velocities. Regarding to salability with fixed bandwidth resource, because of the user request-orientated adaptive subcarrier bandwidth adjustment, ABMA is the compromise of baseline OFDMA ($f_s = 15$ kHz) and adjusted subcarrier bandwidth OFDMA (f_s is fully switched to 30 kHz).

5 Conclusion

In this paper, we propose a downlink multi-user access scheme based on filtered-OFDM waveform, named adaptive subcarrier-bandwidth multiple access (ABMA), targeting at high-mobility environment with different kinds of high-speed receivers. ABMA allows coexistence of difference sizes of subcarrier bandwidth. Frequency-domain quasi-orthogonality is obtained by resource band based filtering. With the time-varying change of user velocities, BS is able to adaptively allocate the spectrum locations and parameters of the resource bands. Adaptation control information is designed, with consideration of adaption flexibility and overhead minimization. With ABMA, ICI power caused by Doppler spread can be limited in a certain range. Simulation results prove the significant gain in BER performance to support a wide range of users with time-varying velocities.

References

1. Schaich, F., Wild, T., Chen, Y.: Waveform contenders for 5G-suitability for short packet and low latency transmissions. In: Proceedings of the 79th Vehicular Technology Conference (VTC Spring), pp. 1–5. IEEE (2014)
2. Abdoli, J., Jia, M., Ma, J.: Filtered OFDM: a new waveform for future wireless systems. In: Proceedings of the 16th International Workshop on Signal Processing Advances in Wireless Communications (SPAWC), pp. 66–70. IEEE (2015)
3. Dong, Z., Fan, P., Hu, Q., Gunther, J., Lei, X.: Filtered OFDM: a new waveform for future wireless systems. IEEE Trans. Veh. Technol. **65**(8), 6038–6050 (2015)
4. Schaich, F., Wild, T.: Subcarrier spacing-a neglected degree of freedom?. In: Proceedings of the 16th International Workshop on Signal Processing Advances in Wireless Communications (SPAWC), pp. 56–60. IEEE (2015)
5. Schaich, F., Wild, T., Ahmed, R.: Subcarrier spacing-how to make use of this degree of freedom. In: Proceedings of the Vehicular Technology Conference (VTC Spring), pp. 1–6, IEEE (2016)
6. Zhang, X., Jia, M., Chen, L., Ma, J., Qiu, J.: Filtered-OFDM-enabler for flexible waveform in the 5th generation cellular networks. In: Proceedings of the Global Communications Conference (GLOBECOM), pp. 1–6. IEEE (2015)
7. Li, Y., Cimini, L.J.: Bounds on the interchannel interference of OFDM in time-varying impairments. IEEE Trans. Commun. **49**(3), 401–404 (2001)
8. Choi, Y., Voltz, P.J., Cassara, F.A.: On channel estimation and detection for multicarrier signals in fast and selective Rayleigh fading channels. IEEE Trans. Commun. **49**(8), 1375–1387 (2001)